Article

Series of In Situ Photo-induced Polymer Graftings for Sensitive Detection of Protein Biomarkers via Cascade Amplification of Liquid Crystal Signals

Xi Wu, Xiaokang Ding, and Fu-Jian Xu

Biomacromolecules, **Just Accepted Manuscript** • DOI: 10.1021/acs.biomac.7b01774 • Publication Date (Web): 05 Feb 2018

Series of In Situ Photo-induced Polymer Graftings for Sensitive Detection of Protein Biomarkers via Cascade Amplification of Liquid Crystal Signals

Xi Wu,[a,b,c] Xiaokang Ding,[a,b,c,*] and Fu-Jian Xu.[a,b,c,*]

[a]State Key Laboratory of Chemical Resource Engineering, Beijing University of Chemical Technology, Beijing 100029 China
[b]Key Laboratory of Carbon Fiber and Functional Polymers (Beijing University of Chemical Technology), Ministry of Education, Beijing 100029 China
[c]Beijing Laboratory of Biomedical Materials, Beijing Advanced Innovation Center for Soft Matter Science and Engineering, Beijing University of Chemical Technology, Beijing 100029 China

*To whom all correspondence should be addressed:

E-mail: dingxk@mail.buct.edu.cn (X.D.); xufj@mail.buct.edu.cn (F.J.X)

ORCID

Xiaokang Ding: 0000-0002-6705-4148

Fu-Jian Xu: 0000-0002-1838-8811

ABSTRACT

Developing of new polymeric materials for the sensitive and rapid detection of trace protein biomarkers has attracted increasing attention in biomedical fields. Herein, series of in situ photo-induced polymer graftings were developed for sensitive detection of protein biomarkers by using featured cascade amplification of liquid crystal (LC) signals. The limit-of-detection (LOD) for native bovine serum albumin (BSA) molecules is around 10 μg/mL in a LC biosensor before signal amplification. Upon the cascade amplification using surface-grafted polymers, poly[poly(ethylene glycol) methacrylate] grafting (*s*-P(PEGMA)) exhibits superior amplification ability (10^4-fold lower than native BSA) than the other two graftings of poly(2-hydroxyethyl methacrylate) (*s*-PHEMA) and poly(methacrylic acid) (*s*-PMAA) (10^2-fold lower than native BSA). The contact angles of water and LC on the *s*-P(PEGMA) grafting show significant difference in comparison with *s*-PHEMA and *s*-PMAA graftings ($p < 0.05$), implying interfacial energies of the grafted polymers may dictate the orientational transition of LCs. The clinical urine samples collected from the patients with proteinuria were also used to confirm the feasibility of the polymer-amplified LC sensors for practical protein assays. The present work reveals that in situ photo-induced polymer grafting is one promising method to amplify the signals of LC biosensors for the rapid and sensitive detection of trace protein biomarkers.

Keywords: photopolymerization, liquid crystal, biosensor, cascade amplification, protein detection

INTRODUCTION

The grafting of polymers on solid substrates has attracted much attention in the past decades due to the versatility in the macromolecular design and the controlling of the interfacial features.[1-3] These polymer-grafted interfaces have found applications in many areas such as the regulation of cell behaviors,[4-6] engineering of hemocompatible[7] and antibacterial coatings,[8-13] and sensing of biomolecules.[14-21] In particular, the grafted polymers in biosensors either provide low-fouling substrates to resist non-specific adsorption of matrix proteins or serve as biointerfaces for the immobilization of antibodies or peptides. For example, the surface-initiated polymer brushes containing polyethylene glycol (PEG) side chains are able to resist non-specific protein adsorption in a surface plasmon resonance imaging biosensor to improve the signal-to-noise ratio.[22] Similarly, a sandwich-type fluorescent immunoassay was reported on a polymer scaffold containing *N*-hydroxysuccinimide groups for immobilization of primary antibodies, while the hydrophobic alkyl or phenyl groups were used to provide anchoring points to cyclic olefin copolymer substrates.[23] Although the above strategies are able to significantly improve the limit-of-detection (LOD) and specificity for the detection of target biomarkers, they require bulky instrumentation to transduce the presence of biomarkers into readable signals.

Liquid crystals (LCs) are birefringent materials widely used in flat panel displays and light regulating devices.[24-27] After the pioneering works of Abbott, LCs have attracted much attention because the presences of biomolecules (proteins or nucleic

acids) are able to disrupt the predefined orientation of LCs.[28-30] Therefore, the biomolecular interactions can be transduced into optical signals that can be easily observed with naked eyes.[31-37] However, the LODs for the detection of biomolecules are in the range of μg/mL, which is insufficient for many clinical assays. Although some attempts have been made by incorporating nanoparticles to enhance the signal amplification,[38] more efforts are still needed to address this problem.

Surface-grafted polymers provided an alternative approach for the amplification of molecular recognition events of biomolecules.[39-41] For example, the dual-functional macrophotoinitiator was synthesized via esterification reaction to incorporate the commercial photoinitiator Irg 2959 into the backbone of poly(acrylic acid-*co*-acrylamide).[40] Meanwhile, the neutravidin molecules were conjugated to the macrophotoinitiators, rendering molecular recognition ability to surface immobilized biotin motifs. After the molecular recognition of neutravidin and biotin motifs, the photopolymerization was subjected and the resultant polymeric materials on the substrate surface can be produced. We propose that this strategy may provide a new approach for the signal amplification of LC biosensors. Herein, to establish a "proof-of-concept" demonstration of using surface-grafted polymers to amplify the signals of LC biosensors, a model protein of bovine serum albumin (BSA) was immobilized on glass slide (Scheme 1). After the bioconjugation of the photo-macroinitiators and the subsequent photo-induced polymer graftings, the LC biosensors would experience cascade signal amplification. This strategy would shed light on how to develop highly sensitive LC-based biosensors for rapid diagnosis of

protein biomarkers.

<Scheme 1>

EXPERIMENTAL SECTION

Materials. Glass slides were purchased from Citotest Labware Manufacturing Co. Ltd. (China). Liquid crystal 4-cyano-4′-pentylbiphenyl (5CB) was purchased from Chengzhi Yonghua Display Material Co. Ltd. (China). Dimethyloctadecyl[3-(trimethoxysilyl)propyl]ammonium chloride (DMOAP) was purchased from Acros Organics (Belgium). Poly(acrylic acid-*co*-acrylamide) (PAAm, Mn: 150 kDa), 2-hydroxy-1-(4-(2-hydroxyethoxy)phenyl)-2-methyl-1-propanon (Irg 2959), and Bradford reagent were purchased from Sigma-Aldrich (USA). Bovine serum albumin (BSA), Decon-90, sodium bicarbonate, magnesium chloride hexahydrate, sodium cyanoborohydride, Tween-20 and 4-(4,6-dimethoxy-1,3,5-triazin-2-yl)-4-methyl morpholinium chloride (DMTMM) were purchased from Energy Chemical (China). Methacrylic acid (MAA), 2-hydroxyethyl methacrylate (HEMA) and poly(ethylene glycol) methacrylate (PEGMA, Mn: 360) were purchased from Tokyo Chemical Industry Co. Ltd. (Japan). Tetrahydrofuran (THF, A.R. grade) was purchased from Beijing Chemical Works (China). Phosphate buffered saline (PBS) buffer (pH 7.4) was reconstituted from PBS salt package purchased from Solarbio (China). The urine samples were collected with informed consent and approval by the Ethics Committee of the Affiliated Hospital of Hebei University.

Synthesis of Photo-Macroinitiator (PAAm-I*). The macroinitiator (PAAm-I*) was synthesized as described elsewhere with a few modifications.[40] Briefly, 10 mL of THF containing 0.5 mol/L of Irg 2959 was added into 30 mL of aqueous solution containing 50 mg/mL of PAAm and 0.17 mol/L of DMTMM in a 100-mL round-bottom flask. After constant stirring for 6 h at 40 °C, the unreacted Irg 2959 and DMTMM were removed by dialysis (MWCO 3500) against deionized water, and the product of macroinitiator (PAAm-I*) was collected after lyophilization.

Protein Immobilization. The glass slides were cleaned with Decon-90 solution (5% v/v) and modified with DMOAP silane as described in our earlier work.[32] Briefly, the cleaned glass slides (*s*-glass) were immersed in an aqueous solution containing 0.4 % v/v of DMOAP silane with gentle rocking. After 5 min, the glass slides were rinsed with deionized water for 3 times to remove unreacted silane. Subsequently, the DMOAP-coated glass slides (*s*-DMOAP) were blown dry under a stream of nitrogen gas and placed in a vacuum oven (100 °C) for 20 min to allow crosslinking of the silanes. Subsequently, the *s*-DMOAP was placed 3 cm below an ultraviolet (UV) pen-lamp (254 nm, Spectroline®, model 11SC-1), and subjected to UV shining for 100 s to promote the formation of aldehyde groups on the glass slide surface (*s*-CHO).[42] Next, 1 μL of the buffer solution (50 mM $NaHCO_3$, 100 mM $MgCl_2$, 10 mM $NaBH_3CN$, pH 10.0) containing different concentrations of BSA (or diluted urine samples obtained from patients with proteinuria) were dispensed on the UV-activated glass surface in an array format. To avoid evaporation of the protein solution, the glass slides were placed in a humidified chamber and incubated at room temperature

(~25 °C) for 3 h. After the protein-immobilized glass slides (*s*-BSA or *s*-protein) were briefly rinsed with deionized water and washed three times with PBS buffer (pH 7.4) containing 0.05% v/v Tween-20 (PBST) to remove the nonspecific adsorption of proteins, the glass slides were blown dry under a stream of nitrogen gas.

In Situ Photopolymerization. To conjugate the macroinitiators (PAAm-I*) to surface-immobilized proteins, the *s*-BSA (or *s*-protein) was incubated in 2 mL of aqueous solution containing PAAm-I* (31.25 mg/mL) and DMTMM (62.5 mg/mL) at room temperature. After 2 h, the glass slides (*s*-initiator) were thoroughly washed with 0.05% v/v PBST to remove the unreacted reagents, and blown dry under a stream of nitrogen gas. For the photopolymerization, the glass slide modified with PAAm-I* (*s*-initiator) was paired with another DMOAP-modified glass slide (*s*-DMOAP) to fabricate a glass cell, separated by two stripes of folded aluminum foil spacers (~50 μm) and secured with two binder clips at the end of two slides. Afterwards, ~100 μL of monomer (HEMA or MAA or PEGMA) was dispensed onto the edge of the glass cell, and the monomer was withdrawn into the empty cavity between the two glass slides to fill up the empty cell by capillary force. Subsequently, the glass cells filled with different monomers were exposed to UV light (365 nm, 4 mW/cm^2). After a period of time (0 – 30 min), the glass cells were disassembled and the glass slides with patterned BSA (or urine proteins) arrays were thoroughly washed with 0.05% v/v PBST for three times to remove unreacted monomers. Finally, the glass slides grafted with polymers (*s*-polymer) were blown dry under a stream of nitrogen gas.

Signal Amplification of the LC Biosensors. The glass slides (*s*-BSA or

s-protein, *s*-initiator, and *s*-polymer) were paired with another DMOAP-modified glass slide (*s*-DMOAP) to fabricate a glass cell, with a fixed distance of ~ 6 μm as defined by the thickness of Mylar film spacers. A drop of 5CB was dispensed onto the edge of the glass cell and the 5CB was withdrawn into the space between the two glass slides to fill up the empty cell by capillary force. The Optical appearance of the sample was observed under a microscope (Leica DM 750P) equipped with crossed polars in the transmission mode. The ratio of the bright (or colorful) areas over a circular sample spot was calculated by using ImageJ (see the Supporting Information). Triplicate samples were calculated to obtain an average value and the standard deviation.

Characterization. The chemical structure of macroinitiator (PAAm-I*) was characterized by ^{1}H NMR spectroscopy (400 MHz, Bruker ARX), using D_2O (δ = 4.8 ppm) as solvent. The amount of initiator moieties in PAAm-I* was determined by UV-Vis spectra (Shimadzu UV-2600), while the amount of total protein in the urine sample was determined by using Bradford assay. The morphologies of the substrates were obtained from an atomic force microscopy (AFM) system (Bruker, Dimension Icon), and the thickness of the films were determined by using scratching method. To obtain viable AFM images, the concentration of BSA used for the surface immobilization is 1 mg/mL, while the other conditions are same as described above. The contact angles of water and 5CB on different films were measured on a contact angle detector (Powereach, China). The concentration of BSA used for the surface immobilization is 10 μg/mL.

Statistical Analysis. The experimental data are presented as means ± standard deviation (SD). Statistical significance ($p < 0.05$) was evaluated using Student's *t*-test when two groups were compared.

RESULTS AND DISCUSSION

Synthesis of Photo-Macroinitiator (PAAm-I*). The macroinitiator (PAAm-I*) was synthesized by esterification reaction between PAAm and Irg 2959 (a commercially available photoinitiator) in the presence of DMTMM (Scheme 1). Figure 1 shows the ^{1}H NMR spectrum of PAAm-I*. The peaks at 8.14 (**a**), 7.12 (**b**), 4.26 (**c**) and 4.01 (**d**) ppm are assigned to Irg 2959. Meanwhile, the peaks at 2.23 (**e**) and 1.67 (**f**) were attributed to the protons in the backbone of PAAm. The ^{1}H NMR spectrum of PAAm-I* is in consistence with that reported in literature.[40] To determine the average number of the Irg 2959 moieties in each macroinitiator, a calibration curve of Irg 2959 was established by measuring the absorbance at 280 nm as a function of concentration (see the Supporting Information). As the absorbance of PAAm-I* (100 μg/mL) is 0.38, we can estimate that about 36.4 Irg 2959 moieties have been immobilized to PAAm-I* (the absorbance of PAAm at 280 nm is minimal). These results, when combined, show that the macroinitiator is successfully synthesized.

<Figure 1>

Morphologies and Thicknesses of the Substrate Surfaces. Figure 2 shows the AFM images of the substrates immobilized with BSA (*s*-BSA), macroinitiator (*s*-initiator), and three different polymers of poly(2-hydroxyethyl methacrylate) (*s*-PHEMA), poly(methacrylic acid) (*s*-PMAA), and poly[poly(ethylene glycol) methacrylate] (*s*-P(PEGMA)), respectively. The images were obtained after scratching a line through the immobilized films to obtain the film thickness. The height profiles

in Figure 2 shows that the immobilized film of BSA is 3.1 nm. After the macroinitiator was conjugated to the BSA, the thickness of the film increased to 5.0 nm, showing that the conjugation of the macroinitiator is successful. After photopolymerization, the thickness of the film increased to 7.2, 7.0, and 7.5 nm, when using HEMA, MAA, and PEGMA as monomers, respectively. We notice that the morphologies and thicknesses of the films are similar among the three samples using different monomers for photopolymerization. To investigate the processes of the growth of the polymer graftings, the thickness of *s*-P(PEGMA) with different UV exposure time were studied by using AFM (see the Supporting Information). With the increasing of UV exposure time, the thickness of the *s*-P(PEGMA) increases from 5.6 nm (5 min) to 6.4 nm (15 min).

<Figure 2>

Cascade Signal Amplification of the LC Biosensors. To investigate the efficacy of the conjugated macroinitiators and the subsequent photopolymerization in amplifying the signal of the LC biosensors, buffer solution containing different concentrations of BSA was dispensed onto the UV-activated glass surface. Figure 3a shows that the LC biosensors only display colorful birefringence when the BSA concentration is 10 μg/mL. When the BSA concentration in the buffer solution is 1 μg/mL or below, the optical appearances of the samples remain dark, showing that the immobilized BSA molecules cannot disrupt the orientation of LCs. After conjugation of the macroinitiator to BSA molecules, the optical appearance of the sample spot immobilized with 1 μg/mL of BSA switches from dark to bright, showing the

conjugation of the macroinitiator is able to improve the LOD of the LC biosensors by 10-fold (Figure 3b). After in situ photopolymerization of PHEMA and PMAA for 30 min, the LOD of the LC biosensors decreased to 100 ng/mL, which is 100-fold lower than the LOD before amplification (Figure 3a), and 10-fold lower than the LOD after one-step amplification by conjugation of the macroinitiators (Figure 3b). More interestingly, after the in situ photopolymerization of P(PEGMA) for 30 min, the LOD of the LC biosensors decreased to 1 ng/mL, which is 10^4-fold lower than the LOD before amplification (Figure 3a), and 10^3-fold lower than the LOD after macroinitiator conjugation. Moreover, the control experiments without DMTMM or without macroinitiator do not trigger optical transition of the LC biosensors (see the Supporting Information). These results indicate the in situ polymer graftings triggered by macroinitiators are able to generate cascade amplification of the optical signals of LC biosensors.

<Figure 3>

As the P(PEGMA) grafted-polymer shows highest signal amplification ability, we further investigate the effect of polymerization time and monomer concentration to the optical appearance of LC biosensors. Figure 4a shows that only the sample spot immobilized with 1 μg/mL of BSA shows colorful birefringence before photopolymerization, while the other sample spots remain dark (Figure 4a1). This result is in consistence with the optical appearance of LC biosensors with macroinitiator conjugation. After the samples are shined with UV light for 5 min, 40.3 ±9.8% in the circular area of the sample spot where immobilized with 100 ng/mL of

BSA switches from dark to bright (Figure 4a2). When the exposure time of UV light extends to 15 min, the ratio of bright areas increases to 64.1±2.4%, suggesting that more P(PEGMA) polymer has been grafted on the glass slide surface. More importantly, 37.7±3.1% of the sample spot immobilized with 10 ng/mL of BSA is bright up (Figure 4a3). These results show that the LOD of LC biosensors decreases with increasing the time of UV light exposure. We also notice that when the UV light exposure time is longer than 45 min, the massive photopolymerization of the monomers would cause severe global stain of the polymers on the glass substrate, which deteriorate the performance of the LC sensors. These results, when combined with the AFM results in Figure 2 and Figure S5, reveal that the signal amplification of the LC biosensors are closely related to the thickness of polymer graftings on the substrate surface. Similarly, Figure 4b shows that with increasing the concentration of PEGMA, the LC biosensors show lower LOD when the UV exposure time is fixed at 30 min.

<Figure 4>

Contact Angles of Water and 5CB. Because it is surprising that the surface-grafted P(PEGMA) shows better abilities in the amplification of the optical signals of LC biosensors, when taking into account that the thickness and morphologies of *s*-PHEMA, *s*-PMAA, and *s*-P(PEGMA) are similar with each other, we decided to investigate the underlying principle that controls the orientational transition of LCs in contact with proteins or grafted-polymers. Figure 5a shows that the water contact angle on *s*-DMOAP is 94.4 ± 1.3°, due to the hydrophobic nature of the long alkyl

chains in DMOAP molecule. After the substrate is immobilized with BSA, the water contact angle decreases to 64.6 ± 1.2°, because the alkyl chains of the DMOAP are partially wrapped by the hydrophilic BSA molecules. After the macroinitiators are conjugated to the BSA molecules, the water contact angle decreases to 53.5 ± 1.2°, showing that more surfaces have been wrapped with hydrophilic macroinitiators. Upon photopolymerization, the resultant water contact angles on *s*-PHEMA and *s*-PMAA decrease slightly to 51.8 ± 1.6° and 52.2 ± 1.0°, respectively. More interestingly, the water contact on *s*-P(PEGMA) is 43.8 ± 1.0°, which has significant difference with the water contact angles on *s*-PHEMA and *s*-PMAA ($p < 0.05$). We propose that this difference confers P(PEGMA) higher signal amplification ability to the LC biosensors compared to PHEMA and PMAA. We also investigated the contact angles of 5CB on *s*-BSA, *s*-initiator, *s*-PHEMA, *s*-PMAA, and *s*-P(PEGMA), respectively. Similar to the water contact angles, the contact angle of 5CB on *s*-P(PEGMA) (14.3 ± 0.4°) also has significant difference with the contact angles of 5CB on *s*-PHEMA (19.9 ± 0.4°) and *s*-PMAA (19.8 ± 0.6°) ($p < 0.05$). These results, when combined, implying that the surface energies of different polymers significantly dictates the orientational transition of LCs on the substrate surfaces.

<Figure 5>

Protein Diagnosis in Clinical Urine Sample. To test the feasibility of the polymer-amplified LC sensors for practical protein assays, the clinical urine samples collected from the patients with proteinuria were sequentially diluted in buffer solution, and immobilized on glass slide in an array format. Figure 6 shows the optical

images of LC biosensors on the substrate of *s*-protein, *s*-initiator, and *s*-P(PEGMA), respectively. The total protein concentration in the urine sample (1.75 ± 0.26 mg/mL) is determined by using Bradford assay (see the Supporting Information). For the glass slides only immobilized with urine proteins (*s*-protein), the sample spots with 10-fold (~175 μg/mL) and 100-fold (~17.5 μg/mL) dilution of the urine sample shows colorful birefringence. This threshold concentration is similar to that of BSA (10 μg/mL). After the conjugation of macroinitiators, the optical appearance of the sample spots with 10^3-fold dilution (~1.75 μg/mL) of the urine sample switches from dark to bright. After photopolymerization for 30 min, the LOD significantly decreased to 10^6-fold dilution (~1.75 ng/mL) of the original urine sample. This "proof-of-concept" demonstration shows that the LC biosensors based on in situ photo-induced polymer graftings are able to quantify total protein concentration in real urine samples.

<Figure 6>

CONCLUSIONS

In conclusion, we demonstrated that series of in situ photo-induced polymer graftings are able to trigger cascade amplification of the LC signals. Compared to native BSA immobilization, the LOD of the LC biosensors was decreased 10-fold after the conjugation of photo-macroinitiators. After photopolymerization, the LOD of the LC biosensors was decreased 100 to 10000-fold. In particular, the graftings of P(PEGMA) show higher amplification than PHEMA and PMAA graftings. We propose that such excellent result is caused by the significant difference of P(PEGMA) in the water/5CB

contact angles compared to those of PHEMA and PMAA. We also demonstrate that the LC sensors based on grafted polymers are able to quantify total protein concentration in real urine samples. The cascade LC signal amplification via in situ photo-induced polymer graftings would benefit the development of more sensitive LC-based biosensors.

ASSOCIATED CONTENT

Supporting Information

Calibration curve of Irg 2959, calibration curve of BSA in Bradford assay, the optical images of LC biosensors without DMTMM or macroinitiator, the calculation of the ratio of bright areas over a circular sample spot, and the AFM images of the substrates of *s*-P(PEGMA) with different UV exposure time.

ACKNOWLEDGES

This work was partially supported by National Key Research and Development Program of China (grant number 2016YFC1100404), National Natural Science Foundation of China (grant numbers 21504006, 51573014, and 51733001), and Beijing Natural Science Foundation (grant number L160004).

References

(1) Barbey, R.; Lavanant, L.; Paripovic, D.; Schüwer, N.; Sugnaux, C.; Tugulu, S.; Klok, H.-A., Polymer Brushes via Surface-Initiated Controlled Radical Polymerization: Synthesis, Characterization, Properties, and Applications. *Chem. Rev.* **2009,** *109*, 5437-5527.

(2) Krishnamoorthy, M.; Hakobyan, S.; Ramstedt, M.; Gautrot, J. E., Surface-Initiated Polymer Brushes in the Biomedical Field: Applications in Membrane Science, Biosensing, Cell Culture, Regenerative Medicine and Antibacterial Coatings. *Chem. Rev.* **2014,** *114*, 10976-11026.

(3) Matyjaszewski, K.; Tsarevsky, N. V., Macromolecular Engineering by Atom Transfer Radical Polymerization. *J. Am. Chem. Soc.* **2014,** *136*, 6513-6533.

(4) Zhang, H.; Wang, D.; Lin, X.; Politakos, N.; Tuninetti, J. S.; Moya, S. E.; Gao, C., Fabrication of Uv Responsive Micelles-Containing Multilayers and Their Influence on Cell Adhesion. *Sci. China Chem.* **2018,** *61*, 54-63.

(5) Liu, H.; Wang, S., Poly(N-Isopropylacrylamide)-Based Thermo-Responsive Surfaces with Controllable Cell Adhesion. *Sci. China Chem.* **2014,** *57*, 552-557.

(6) Leigh, B. L.; Cheng, E.; Xu, L.; Andresen, C.; Hansen, M. R.; Guymon, C. A., Photopolymerizable Zwitterionic Polymer Patterns Control Cell Adhesion and Guide Neural Growth. *Biomacromolecules* **2017,** *18*, 2389-2401.

(7) Luan, S.; Zhao, J.; Yang, H.; Shi, H.; Jin, J.; Li, X.; Liu, J.; Wang, J.; Yin, J.; Stagnaro, P., Surface Modification of Poly(Styrene-*b*-(Ethylene-*co*-Butylene)-*b*-Styrene) Elastomer via UV-Induced Graft Polymerization of N-Vinyl Pyrrolidone. *Colloids Surf., B* **2012,** *93*, 127-134.

(8) Wei, T.; Zhan, W.; Yu, Q.; Chen, H., Smart Biointerface with Photoswitched Functions between Bactericidal Activity and Bacteria-Releasing Ability. *ACS Appl. Mater. Interfaces* **2017,** *9*, 25767-25774.

(9) Wei, T.; Tang, Z.; Yu, Q.; Chen, H., Smart Antibacterial Surfaces with Switchable Bacteria-Killing and Bacteria-Releasing Capabilities. *ACS Appl. Mater. Interfaces* **2017,** *9*, 37511-37523.

(10) Wu, C.; Schwibbert, K.; Achazi, K.; Landsberger, P.; Gorbushina, A.; Haag, R., Active Antibacterial and Antifouling Surface Coating via a Facile One-Step Enzymatic Cross-Linking. *Biomacromolecules* **2017,** *18*, 210-216.

(11) Yan, S.; Luan, S.; Shi, H.; Xu, X.; Zhang, J.; Yuan, S.; Yang, Y.; Yin, J., Hierarchical Polymer Brushes with Dominant Antibacterial Mechanisms Switching from Bactericidal to Bacteria Repellent. *Biomacromolecules* **2016,** *17*, 1696-1704.

(12) Pranantyo, D.; Xu, L. Q.; Neoh, K.-G.; Kang, E.-T.; Ng, Y. X.; Teo, S. L.-M., Tea Stains-Inspired Initiator Primer for Surface Grafting of Antifouling and Antimicrobial Polymer Brush Coatings. *Biomacromolecules* **2015,** *16*, 723-732.

(13) Yan, S.; Shi, H.; Song, L.; Wang, X.; Liu, L.; Luan, S.; Yang, Y.; Yin, J., Nonleaching Bacteria-Responsive Antibacterial Surface Based on a Unique Hierarchical Architecture. *ACS Appl. Mater. Interfaces* **2016,** *8*, 24471-24481.

(14) Wu, Y.; Wang, A.; Ding, X.; Xu, F.-J., Versatile Functionalization of Poly(Methacrylic Acid) Brushes with Series of Proteolytically Cleavable Peptides for Highly Sensitive Protease Assay. *ACS Appl. Mater. Interfaces* **2017,** *9*, 127-135.

(15) Wakabayashi, R.; Yahiro, K.; Hayashi, K.; Goto, M.; Kamiya, N., Protein-Grafted Polymers Prepared through a Site-Specific Conjugation by Microbial Transglutaminase for an Immunosorbent Assay. *Biomacromolecules* **2017,** *18*, 422-430.

(16) Bilgic, T.; Klok, H.-A., Oligonucleotide Immobilization and Hybridization on Aldehyde-Functionalized Poly(2-Hydroxyethyl Methacrylate) Brushes. *Biomacromolecules* **2015,** *16*, 3657-3665.

(17) Ma, J.; Luan, S.; Song, L.; Yuan, S.; Yan, S.; Jin, J.; Yin, J., Facile Fabrication of Microsphere-Polymer Brush Hierarchically Three-Dimensional (3D) Substrates for Immunoassays. *Chem. Commun.* **2015,** *51*, 6749-6752.

(18) Ma, J.; Luan, S.; Song, L.; Jin, J.; Yuan, S.; Yan, S.; Yang, H.; Shi, H.; Yin, J., Fabricating a Cycloolefin Polymer Immunoassay Platform with a Dual-Function Polymer Brush via a Surface-Initiated Photoiniferter-Mediated Polymerization Strategy. *ACS Appl. Mater. Interfaces* **2014,** *6*, 1971-1978.

(19) Tugulu, S.; Arnold, A.; Sielaff, I.; Johnsson, K.; Klok, H. A., Protein-Functionalized Polymer Brushes. *Biomacromolecules* **2005,** *6*, 1602-1607.

(20) Qian, H.; He, L., Surface-Initiated Activators Generated by Electron Transfer for Atom Transfer Radical Polymerization in Detection of DNA Point Mutation. *Anal. Chem.* **2009,** *81*, 4536-4542.

(21) Qian, H.; He, L., Detection of Protein Binding Using Activator Generated by Electron Transfer for Atom Transfer Radical Polymerization. *Anal. Chem.* **2009,** *81*, 9824-9827.

(22) Hu, W.; Liu, Y.; Lu, Z.; Li, C. M., Poly[Oligo(Ethylene Glycol) Methacrylate-*co*-Glycidyl Methacrylate] Brush Substrate for Sensitive Surface Plasmon Resonance Imaging Protein Arrays. *Adv. Funct. Mater.* **2010,** *20*, 3497-3503.

(23) Sung, D.; Shin, D. H.; Jon, S., Toward Immunoassay Chips: Facile Immobilization of Antibodies on Cyclic Olefin Copolymer Substrates through Pre-Activated Polymer Adlayers. *Biosens. Bioelectron.* **2011,** *26*, 3967-3972.

(24) Wang, M.; Zou, C.; Sun, J.; Zhang, L.; Wang, L.; Xiao, J.; Li, F.; Song, P.; Yang, H., Asymmetric Tunable Photonic Bandgaps in Self-Organized 3D Nanostructure of Polymer-Stabilized Blue Phase I Modulated by Voltage Polarity. *Adv. Funct. Mater.* **2017,** *27*, 1702261.

(25) Liang, X.; Chen, M.; Guo, S.; Zhang, L.; Li, F.; Yang, H., Dual-Band Modulation of Visible and Near-Infrared Light Transmittance in an All-Solution-Processed Hybrid Micro–Nano Composite Film. *ACS Appl. Mater. Interfaces* **2017,** *9*, 40810-40819.

(26) Sun, Y.; Zhang, C.; Cao, H.; Xiao, J.; Ding, H.; Li, F.; Yu, H.; Yang, Z.; Yang, H., Effects of Functionality of Thiol Monomer on Electro-Optical Properties of Polymer-Dispersed Liquid Crystal Films. *Liq. Cryst.* **2017,** *44*, 1086-1092.

(27) Chen, Y.; Yu, H.; Zhang, L.; Yang, H.; Lu, Y., Photoresponsive Liquid Crystals Based on Halogen Bonding of Azopyridines. *Chem. Commun.* **2014,** *50*, 9647-9649.

(28) Brake, J. M.; Daschner, M. K.; Luk, Y. Y.; Abbott, N. L., Biomolecular Interactions at Phospholipid-Decorated Surfaces of Liquid Crystals. *Science* **2003,** *302*, 2094-2097.

(29) Gupta, V. K.; Skaife, J. J.; Dubrovsky, T. B.; Abbott, N. L., Optical Amplification of Ligand-Receptor Binding Using Liquid Crystals. *Science* **1998,** *279*, 2077-2080.

(30) Shah, R. R.; Abbott, N. L., Principles for Measurement of Chemical Exposure Based on Recognition-Driven Anchoring Transitions in Liquid Crystals. *Science* **2001,** *293*, 1296-1299.

(31) Chen, C. H.; Yang, K. L., Oligopeptide Immobilization Strategy for Improving Stability and Sensitivity of Liquid-Crystal Protease Assays. *Sens. Actuators, B* **2014,** *204*, 734-740.

(32) Ding, X.; Yang, K. L., Antibody-Free Detection of Human Chorionic Gonadotropin by Use of Liquid Crystals. *Anal. Chem.* **2013,** *85*, 10710-10716.

(33) Lai, S. L.; Tan, W. L.; Yang, K. L., Detection of DNA Targets Hybridized to Solid Surfaces Using

Optical Images of Liquid Crystals. *ACS Appl. Mater. Interfaces* **2011,** *3*, 3389-3395.

(34) Liu, Y.; Yang, K. L., Applications of Metal Ions and Liquid Crystals for Multiplex Detection of DNA. *J. Colloid Interface Sci.* **2015,** *439*, 149-153.

(35) Ong, L. H.; Yang, K. L., Surfactant-Driven Assembly of Poly(Ethylenimine)-Coated Microparticles at the Liquid Crystal/Water Interface. *J. Phys. Chem. B* **2016,** *120*, 825-833.

(36) Xue, C. Y.; Yang, K. L., Dark-to-Bright Optical Responses of Liquid Crystals Supported on Solid Surfaces Decorated with Proteins. *Langmuir* **2008,** *24*, 563-567.

(37) Zhu, Q. D.; Trau, D., Multiplex Detection Platform for Tumor Markers and Glucose in Serum Based on a Microfluidic Microparticle Array. *Anal. Chim. Acta* **2012,** *751*, 146-154.

(38) Zhao, D.; Peng, Y.; Xu, L.; Zhou, W.; Wang, Q.; Guo, L., Liquid-Crystal Biosensor Based on Nickel-Nanosphere-Induced Homeotropic Alignment for the Amplified Detection of Thrombin. *ACS Appl. Mater. Interfaces* **2015,** *7*, 23418-23422.

(39) Sikes, H. D.; Jenison, R.; Bowman, C. N., Antigen Detection Using Polymerization-Based Amplification. *Lab Chip* **2009,** *9*, 653-656.

(40) Sikes, H. D.; Hansen, R. R.; Johnson, L. M.; Jenison, R.; Birks, J. W.; Rowlen, K. L.; Bowman, C. N., Using Polymeric Materials to Generate an Amplified Response to Molecular Recognition Events. *Nat. Mater.* **2008,** *7*, 52-56.

(41) Kaastrup, K.; Sikes, H. D., Polymerization-Based Signal Amplification under Ambient Conditions with Thirty-Five Second Reaction Times. *Lab Chip* **2012,** *12*, 4055-4058.

(42) Liu, Y. Y.; He, J. Z.; Yang, K. L., DNA Microarrays on Ultraviolet-Modified Surfaces for Speciation of Bacteria. *Anal. Biochem.* **2014,** *447*, 156-161.

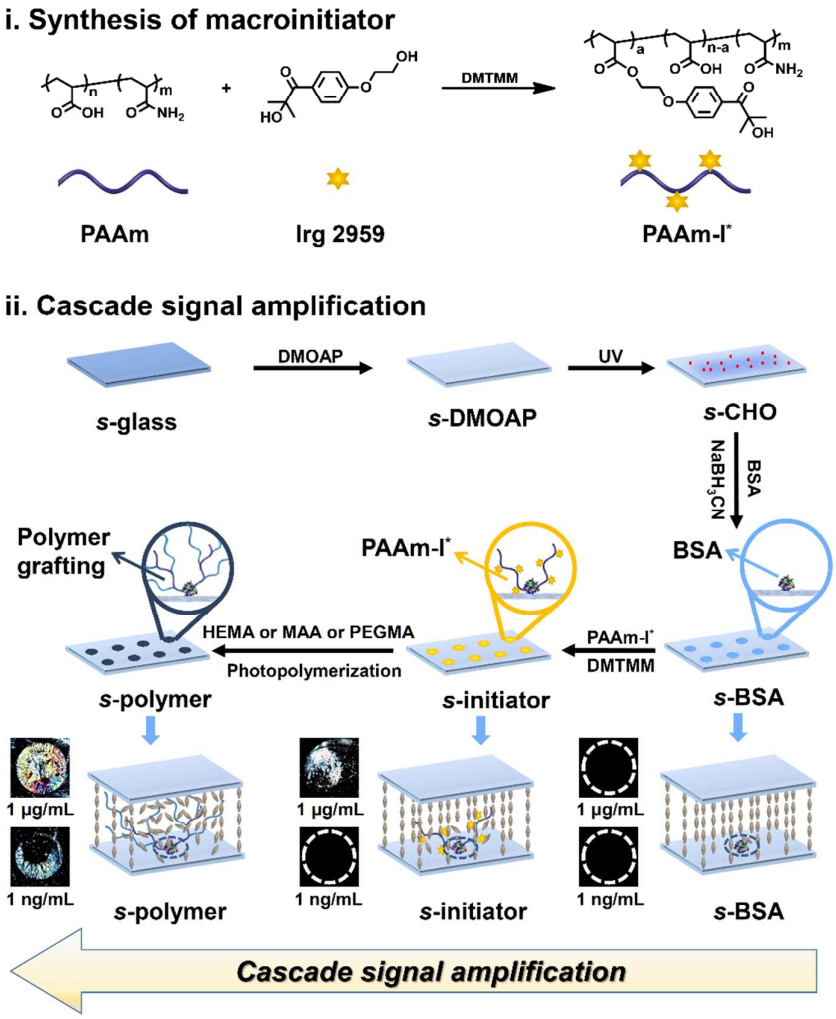

Scheme 1. Schematic illustration of the macroinitiator preparation and liquid crystal based cascade signal amplification for protein detection.

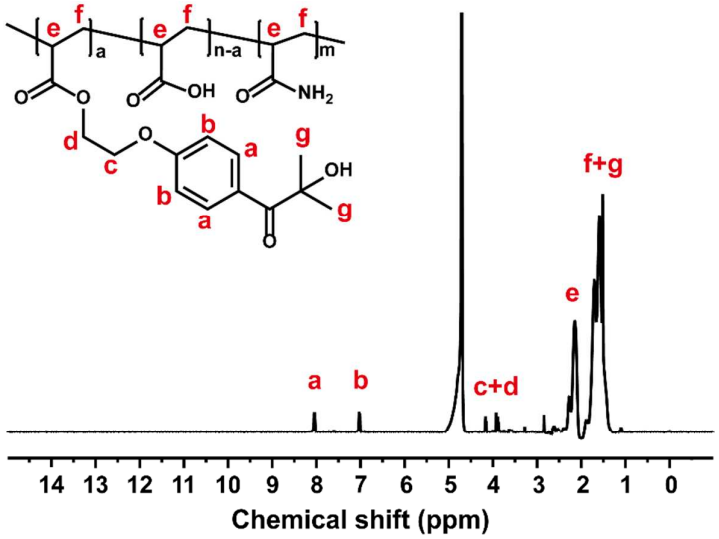

Figure 1. ^{1}H NMR spectrum of the macroinitiator PAAm-I*.

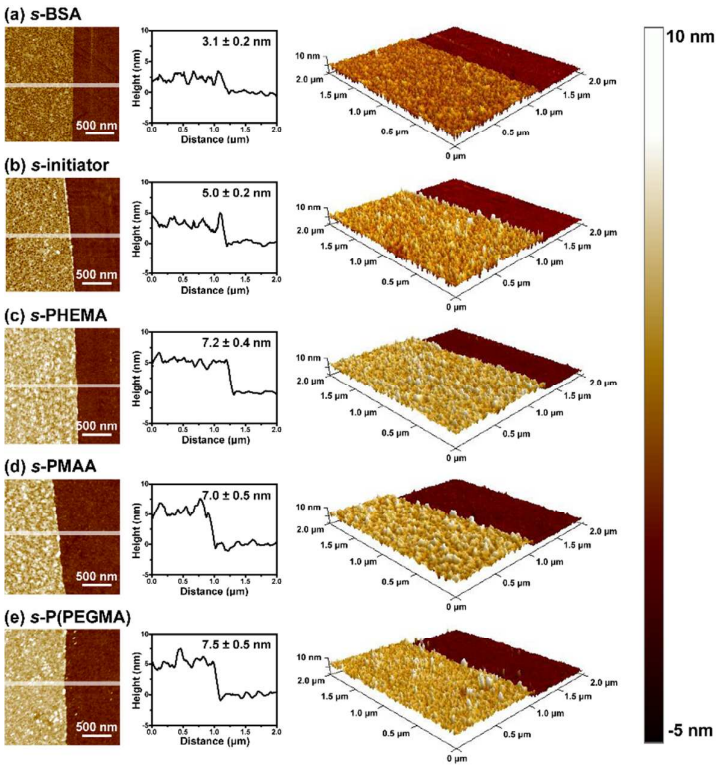

Figure 2. AFM images of the substrates of (a) *s*-BSA, (b) *s*-initiator, (c) *s*-PHEMA, (d) *s*-PMAA, and (e) *s*-P(PEGMA). The first column shows the morphologies of the substrate surfaces (left) at the vicinity of the scratching line (right). The second column shows the height profiles of the substrate surfaces along with the white line. The third column shows the 3-dementional profiles of the substrate surfaces.

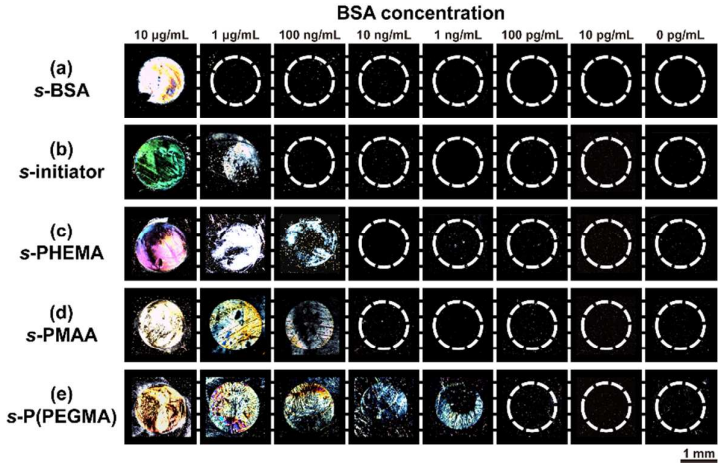

Figure 3. Optical images of the LC biosensors on the substrate of (a) *s*-BSA, (b) *s*-initiator, (c) *s*-PHEMA, (d) *s*-PMAA, and (e) *s*-P(PEGMA), respectively. The BSA concentration was indicated above each column.

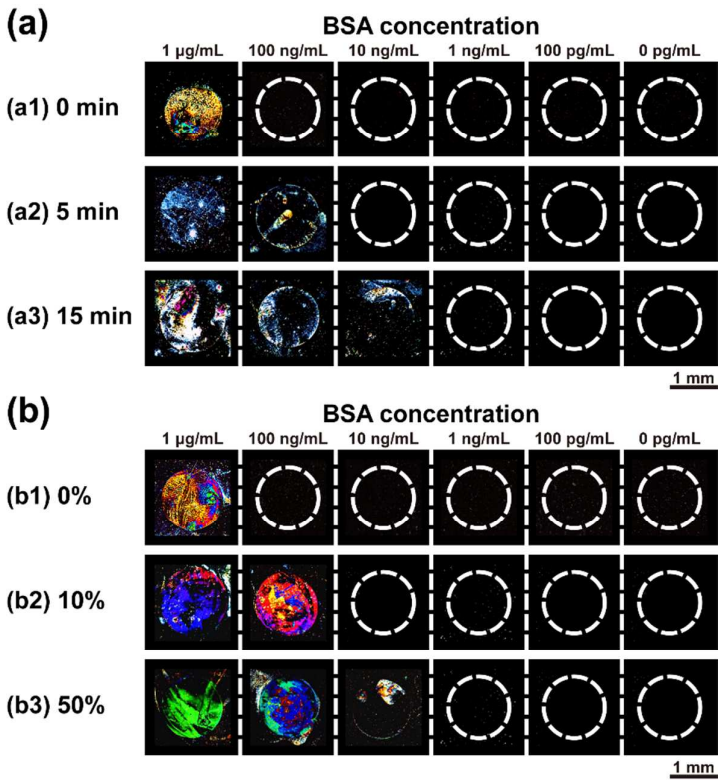

Figure 4. Optical images of LC biosensors on the substrate of *s*-P(PEGMA) with (a) different photopolymerization time, and (b) different concentrations of PEGMA monomer.

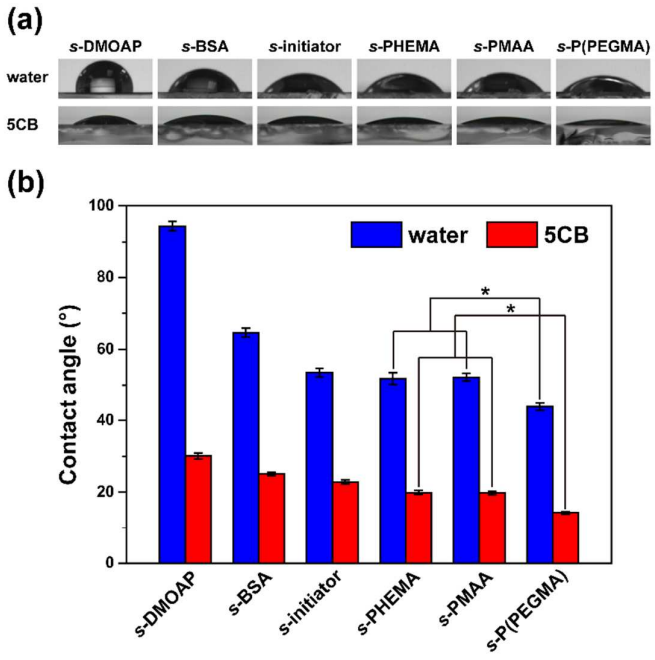

Figure 5. (a) Images and (b) statistical analysis (* $p < 0.05$) of the contact angles of water and 5CB on the substrates of *s*-DMOAP, *s*-BSA, *s*-initiator, *s*-PHEMA, *s*-PMAA, and *s*-P(PEGMA), respectively.

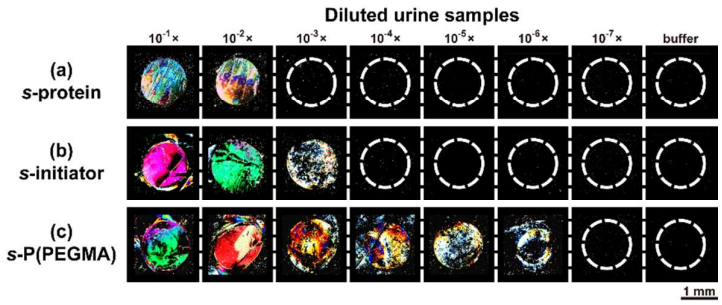

Figure 6. Optical images of LC biosensors for total protein assay of the clinical urine samples on the substrates of (a) *s*-protein, (b) *s*-initiator, and (c) *s*-P(PEGMA), respectively.

Table of contents (TOC)